ELSEVIER

Polymer 44 (2003) 1589–1594

polymer

www.elsevier.com/locate/polymer

On the processability of metallocene-catalysed polyethylene: effects of blending with ethylene–vinyl acetate copolymer

J. Peón[a], M. Aguilar[a], J.F. Vega, B. del Amo[a,b], J. Martínez-Salazar[a,*]

[a]*GIDEM, Instituto de Estructura de la Materia, CSIC, Serrano 113-123, 28006 Madrid, Spain*
[b]*Repsol I + D, Embajadores 183, 28045 Madrid, Spain*

Received 7 August 2002; received in revised form 10 December 2002; accepted 21 December 2002

Abstract

The rheological properties of metallocene-catalysed linear polyethylenes and those of blends prepared with ethylene–vinyl acetate copolymers were evaluated. The pure polyethylenes showed characteristic features of linear polymers in the melt state, but poor processability, as would be expected for materials of narrow molecular weight distribution. The characteristic sharkskin and slip-stick regimes appear at around 0.16 and 0.35 MPa, respectively, during extrusion. Blending polyethylene with ethylene/vinyl acetate copolymers gave rise to smooth extrusion for a characteristic blend composition. The linear viscoelastic response of the blends revealed the behaviour of heterogeneous emulsion-like polymer systems. Through the application of several rheological criteria, we were able to locate the phase inversion concentration of the system. This concentration was found to closely correspond to that at which distortion regimes disappear during extrusion.

Keywords: Metallocene polyethylene; Blends; Viscoelastic properties

1. Introduction

Distortion is a common feature of the extrusion process in polymeric materials such as linear polyethylenes and polypropylenes synthesised through metallocene catalyst systems [1–6]. Measures aimed at avoiding these irregularities include specially designed orifices (alternative materials [7], fluorinated surfaces [8] and the use of porous media at the entrance of the orifice [9]), blending with branched [10] or liquid crystalline [11] polymers, and processing at temperatures just above the melting point [12,13]. In addition, blending additives are often used in the polymer industry to help process polymer melts. Chemical additives, such as fluorelastomers and organosilicon compounds, and boron nitride [14], attempt to minimise surface roughness in polymer processing.

The origin of distortion in the extrudate has been the subject of some dispute [15]. Initially, it was established that distortions are the result of a crack formation mechanism provoked by the action of high tensile stresses that may develop at the exit-die region [16,17]. According to this theory, Cogswell noted that the surface layer of the melt near the wall broke above a certain critical value of the extrudate velocity [18]. This idea is still supported by recent findings reported by El Kissi et al. [19] and numerical simulations by Rutgers and Mackey [20].

A completely different rationale links the appearance of these defects with a wall slip at the polymer–wall interface [7,21,22]. This theory has been put to the test using models designed to take into account chain stretching during the detachment process from the wall [23,24]. A more recent approach by Brochard and de Gennes [25], considers coil-stretch transition of grafted chains from the bulk, i.e. a disentanglement mechanism, as the main cause of slip phenomena. Also based on this concept, Wang and co-workers postulated the possibility of a double mechanism: chain disentanglement and adhesive failure for weakly adsorbed species at the wall orifice [26,27]. This has been called the interfacial molecular instability mechanism (IMI). However, by examining flow behaviour in the immediate vicinity of the exit of the capillary die, it has

* Corresponding author. Address: GIDEM, Instituto de Estructura de la Materia, CSIC, Serrano 113-123, 28006 Madrid, Spain. Tel.: +34-915901618; fax: +34-915855413.
E-mail address: jmsalazar@iem.cfmac.csic.es (J. Martínez-Salazar).

0032-3861/03/$ - see front matter © 2003 Elsevier Science Ltd. All rights reserved.
PII: S0032-3861(02)00941-2

been recently shown that stick, slip and oscillating slip-stick boundary conditions can occur during sharkskin processes [28]. This means that the cause of sharkskin is unconnected to the boundary condition at the polymer/wall interface but to the flow conditions just beyond the exit. Migler [28] has recently suggested that the sharkskin phenomenon is caused by tearing of the polymer because of the high extensional stress suffered by the material just beyond the exit point at the polymer–air interface.

We recently demonstrated that the addition of ethylene/-vinyl acetate copolymer (EVAc) to polyethylene (PE) greatly improves its rheological properties in terms of elasticity [29]. The heterogeneous morphology of these blends gives rise to extra-storage of elastic energy mechanisms due to interfacial phenomena between the phases during shear thinning. This could eventually lead to improved melt properties of potential interest in industrial applications such as blow moulding. In this paper we explore the effects of adding EVAc to a metallocene-catalysed polyethylene (mPE) known to be poorly processed on extrusion. The results obtained were compared to those previously recorded for a family of linear mPEs [13].

2. Experimental

2.1. Materials and blend preparation

mPE and EVAc samples were supplied by Repsol-YPF, Spain. The properties of the polymers are presented in Table 1. The reader is referred to our previous works for details of the characterisation methods used [30,31]. Blending between mPE1 and EVAc was carried out in an internal mixer Brabender Plasticorder fitted with a cam type rotor. The temperature was set at 160 °C, and the torque at 15 Nm. Mixing was performed for about 5 min until the torque and speed rotor had stabilised. The blends were denoted mPE*w*, where *w* is the weight fraction of mPE in the mixture. The mixed mass was compression moulded for 2 min at 160 °C in a Schwabenthan Polystat 200 T and a nominal pressure of 150 bar, and then quenched at room temperature. Disk specimens 25 mm in diameter were stamped for dynamic torsion measurements. The thickness of the compression-moulded samples was adjusted for the rheological measurements. The pure materials were treated in the same way.

Table 1
Molecular characterisation of the materials: vinyl acetate content, weight-average molecular weight, polydispersity index and branching content

Sample	% VAc	M_w	M_w/M_n	SCB ≤ 6C[c]	LCB > 6C[c]
mPE1	–	180000	2.0	0	0
mPE2	–	152000	2.3	0	0
mPE3	–	118200	2.2	10.7	0
EVAc	27.0	91100	3.9	5.5	<0.5

2.2. Melt rheology

Linear viscoelastic measurements were performed using a stress control Bohlin CVO torsion rheometer fitted with 25 mm diameter stainless steel parallel plates and cone–plate geometries. The angular frequency dependence of linear viscoelastic functions, storage modulus G', loss modulus G'', and complex viscosity η^*, were determined at a temperature of 160 °C in the frequency range 10^{-3}–10^2 rad s^{-1}. All tests were performed at a maximum strain of 15%, which was within the linear range for all the samples tested. The gap between parallel plates was set at 0.50 mm for all measurements. Measurements were repeated several times on the same and on fresh samples to avoid blending shear history and degradation effects. In each case, variation among measurements was negligible.

The pure materials and mixtures were subjected to extrusion in the non-linear regime in a piston-type capillary rheometer CEAST rheoscope 1000 over the shear rate range of 6–2400 s^{-1}. Capillary die length and diameter were 40 and 1 mm, respectively. We can consider the capillary die long enough to avoid the Bagley correction. The shear rate was corrected using the conventional expressions of the Rabinowitsch method. The melt temperature was kept at 160 °C. Individual extrudate samples were collected at each shear rate and cooled at room temperature. The physical appearance of extrudates was also compared by visual inspection.

3. Results and discussion

3.1. Rheological properties of the blends

Fig. 1 shows the angular frequency ω dependence of the storage modulus $G'(\omega)$ at 160 °C for some of the blends examined. Particularly at low frequencies, these blends show a characteristic change in the slope $G'(\omega)$, such as that observed in phase-separated systems. This change clearly indicates specific interactions between the two components, also manifested in the system's viscoelastic properties [32].

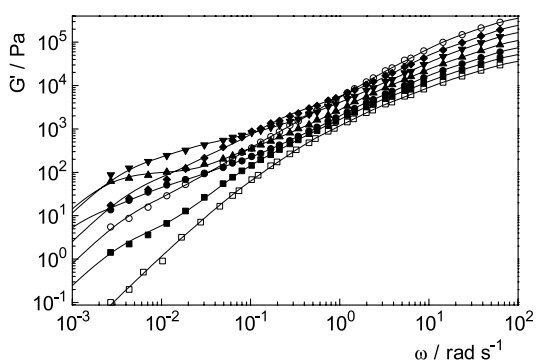

Fig. 1. Storage modulus G' versus angular frequency ω at 160 °C for the pure materials and some of the blends: (□) EVAc, (■) mPE020, (●) mPE040, (▲) mPE050, (▼) mPE060 (◆) mPE080 and (○) mPE1.

This behaviour was attributed to a super-slow relaxation process, typically considered as being an indication of droplet deformation–relaxation dynamics in immiscible blends. This particular issue has been addressed in a separate paper [29]. Striking behaviour was also shown by the complex viscosity $\eta^*(\omega)$, which displayed a clear inflexion point at the lowest frequencies (Fig. 2). This figure also includes steady-state viscosities $\eta(\dot{\gamma})$ obtained from the extrusion capillary measurements, assuming the Cox–Merz rule holds [33]:

$$\eta(\dot{\gamma}) = |\eta^*(\omega)|_{\dot{\gamma}=\omega} \quad (1)$$

It can be clearly seen that steady-state viscosity $\eta(\dot{\gamma})$ and complex viscosity $\eta^*(\omega)$ are of the same order of magnitude, yet they show a difference of around 15%. The Cox–Merz rule has been always thought to be empirical, since it correlates linear and non-linear functions. In a recent theoretical study, however, this rule was validated by considering double reptation as the primary mechanism of stress relaxation [34]. For blends, fulfilment of the rule has always been regarded as a requisite for assessing homogeneity. However, it cannot be taken as proof of homogeneity [35].

The behaviour of heterogeneous blends in the phase inversion region is of notable interest. Several rheological criteria may be used to locate the volume phase inversion concentration ϕ_{dI} in this type of blend. At this concentration the low frequency zone usually shows the following features: (i) maximum dynamic viscosity η' values; (ii) maximum storage modulus G' values; and (iii) minimum G' slopes [36]. The results of applying these criteria to our blends at the lowest accessible frequency are shown in Table 2. We considered the weight w and volume ϕ fractions to be equal, i.e. both components were assumed to have the same melt density ρ. It may be clearly seen, that methods (i) and (ii) locate phase inversion composition at around $w = 0.60$, while criterion (iii) locates it at the lower value of $w = 0.50$.

Utracki [37] proposed a criterion based on the Krieger and Dougherty model [38] that evokes the idea that co-continuity is associated with maximum viscous extra

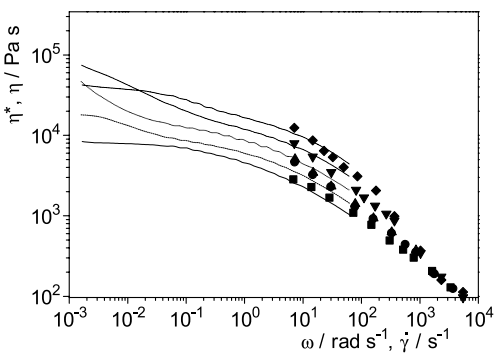

Fig. 2. Cox–Merz rule for some of the blends at 160 °C. Symbols the same as for Fig. 1. Lines: dynamic measurements; symbols: extrusion measurements

Table 2
Rheological criteria ($\omega = 0.0027$ rad s^{-1}) recorded at a temperature of 160 °C to locate phase inversion composition

Sample	η' (Pa s)	G' (Pa)	G' slope
EVAc	4900	0.102	1.9
mPE010	6300	0.274	1.7
mPE020	8100	1.43	1.2
mPE030	11100	3.69	1.1
mPE040	16670	13.6	0.96
mPE050	25320	62.5	0.34[a]
mPE060	54720[a]	87.6[a]	0.67
mPE070	41400	78.9	1.1
mPE080	40050	17.2	1.1
mPE090	35100	10.9	1.1
mPE1	33000	5.48	1.2

[a] These values locate the phase inversion concentration (see text).

stresses. Krieger and Dougherty derived an expression for blend viscosity, dependent on the viscosity of the matrix η_m, the volume fraction of the second component ϕ, the maximum package fraction, ϕ_M and the intrinsic viscosity $[\eta]$:

$$\eta = \eta_m\left(1 - \frac{\phi}{\phi_M}\right)^{-[\eta]\phi_M} \quad (2)$$

The rationale behind Utracki's relation for immiscible polymer blends, was that the composition at which the viscosity function takes its maximum value is an isoviscous point. This point corresponds to the composition ϕ_{dI} at which adding polymer 2 to polymer 1 and viceversa, viscosity shares a common value, and phase inversion takes place. If one defines K as the viscosity ratio of the components of the blend, then it follows from Eq. (2) that (see Ref. [37]):

$$K = \left[\frac{(\phi_M - \phi_{dI})}{\phi_M - (1 - \phi_{dI})}\right]^{-[\eta]\phi_m} \quad (3)$$

Relation 3 has been tested for a large number of immiscible blends, yielding $[\eta] = 1.9$ and $\phi_M = 0.84$ [37]. In our case, a slightly higher value of $\phi_{dI} = w_{dI} = 0.68$ was obtained but this value was in close agreement with that achieved by means of criteria (i) and (ii). Fig. 3 presents a comparison of the use of all the criteria defined above to predict phase inversion in our blends; results were fairly consistent and phase inversion composition was located at around $w = 0.60$.

3.2. Sample appearance and processability

3.2.1. (a) Characteristic distortion regimes

Fig. 4 shows flow curves of the pure materials determined at 160 °C. The sharkskin regime, characterised by high frequency, small-amplitude periodic distortion along the extrudate surface, can be observed for the mPEs, provided a critical value of shear stress of about $\sigma_{c1} = 0.16$ MPa is reached. This value, which has been

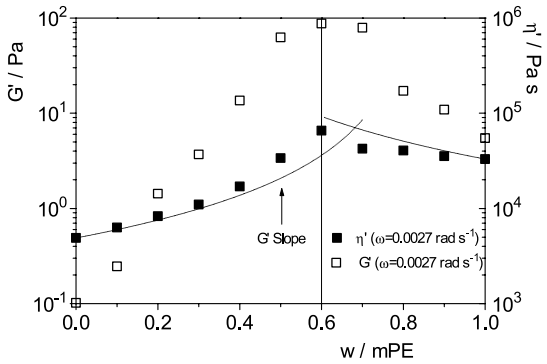

Fig. 3. Rheological criteria used to locate the phase inversion composition: (■) η' values at 0.0027 rad s^{-1}, (□) G' values at 0.0027 rad s^{-1}. Vertical solid line indicates the phase inversion composition obtained by means criteria (i) and (ii), and the arrow represents the phase inversion composition obtained by means criterion (iii) (see text). The dashed line shows the Krieger and Dougherty model estimation of phase inversion composition (Eqs. (2) and (3)).

reported to be independent of temperature, M_w and short chain branching (SCB) content, is well inside the limiting values cited in the literature for linear PE [13,26,27,39], generally in the range 0.1–0.2 MPa. A second distortion regime, at a shear stress of around $\sigma_{c2} = 0.35$ MPa was also observed for the mPEs. At this critical value, slip-stick transition reflected by sudden oscillations in the extrusion pressure and the appearance of alternatively smooth and rough or 'bamboo-like' extrudates takes place. The morphological details of the cooled extrudates of the mPEs studied in the sharkskin region, such as those shown in Fig. 5, were examined. Extrudates were obtained at 160 °C under similar values of shear stress, 0.31–0.35 MPa, just before the slip-stick transition. It can be observed that the sharkskin distortion takes the form of a perfect periodic helix. This distortion is characterised by a periodicity, τ, defined by the ratio λ/V, where λ is the wavelength between neighbouring ridges and V the linear velocity of the extrudate. Periodicity values were calculated according to the procedure described by Wang et al. [26,27]. Sharkskin periodicity can be defined as a function of the

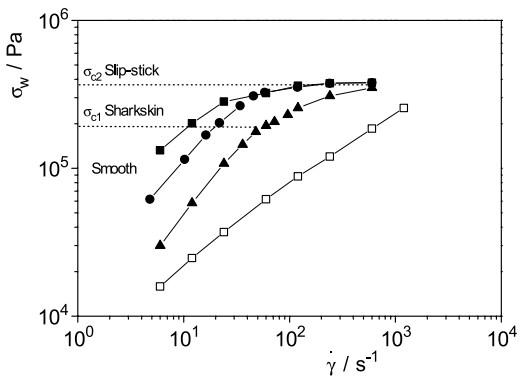

Fig. 4. Uncorrected flow curves of shear stress versus shear rate at 160 °C for the pure polymers: (■) mPE1, (●) mPE2, (▲) mPE3 and (□) EVAc. The dashed horizontal lines indicate the critical stress values for the onset of the characteristic distortion regimes in mPEs.

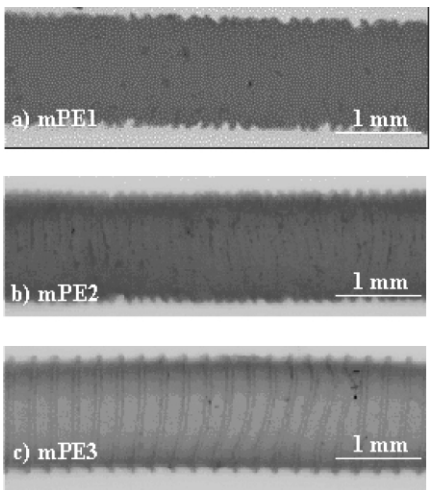

Fig. 5. Micrographs of polymer extrudates taken at $T = 160$ °C and $\sigma = 0.31$–0.33 MPa below the slip-stick transition, (a) mPE1, (b) mPE2, (c) mPE3.

sharkskin wavelength between neighbouring ridges λ, the die swell ratio dj/D, and the shear rate $\dot{\gamma}$:

$$\tau = \frac{8\lambda}{D\left(\frac{D}{\mathrm{dj}}\right)^2 \dot{\gamma}} \tag{4}$$

When compared with results obtained in similar conditions of stress and temperature for a series of mPEs [13,39,40], the periodicity values obtained here were of the same order of magnitude (around 0.01).

The EVAc, on the other hand, show neither the sharkskin nor the slip-stick regime. These copolymers yield smooth extrudates across the entire range of shear covered in the experiments. It is known that EVA copolymers are long chain branched polymers [31]. Long chain branched polyolefins show comparable results in extrusion experiments [1–3]. Contrary to linear mPEs, which present relatively low relaxation times possibly sufficient for macromolecules to become entangled and disentangled in the extrusion experimental time window, branched polymers are characterised by larger relaxation times due to the presence of long branches. Thus, the IMI model may account for the vanishing of distortions when the extrusion time frame is such that there is insufficient time for the coil-stretch mechanism to proceed. On the other hand the extrudate surface cracking evoked by Cogswell [18] and more recently by Migler [28] is also able to explain the elimination of distortions, regardless of conditions at the polymer/wall interface. Distortion is not always a feature of branched polymers such as low-density polyethylene (LDPE) and EVAc [41], in which chain branching is generally thought to delay chain dynamics [42], causing enhanced elasticity and melt strength [43,44], and thus resistance to tearing. We could also try another possible explanation. Materials with relatively low entanglement density are less susceptible to a coil-stretch transition [45]. It

is then possible to assume that the entanglement density of EVAc could be lower than that of linear mPE. Unfortunately, it is very difficult to measure in long chain branched polymers a rheological property directly related to the entanglement density such as the plateau modulus, G_N^0 [30]. At this point of the discussion it is worthwhile to mention that a decrease of the entanglement density does not always lead to the elimination of the extrudate distortions, as it has been recently observed in ethylene/1-hexene copolymers [46]. In fact it seems that in these materials, with a low entanglement density, distortions appear even at a lower stress level. Also other linear polymers as poly(dimethylsiloxane) (PDMS), characterised by a low entanglement density (comparable to that corresponding to polystyrene, which certainly does not show instabilities) are known to present distortions during extrusion [47].

The subject is a complex issue and it is beyond the scope of this paper to further discuss the origin of this important feature of polymer melts. The following results will be considered in the context of another interesting phenomenon: eliminating distortion.

3.2.2. (b) Effect of blending on processability

Fig. 6 shows flow curves of the blends determined at 160 °C. The sharkskin regime can only be observed in mPE1 and in blend compositions higher than $w = 0.70$, provided a critical value of shear stress around $\sigma_{c1} = 0.16$ MPa is reached. At a constant shear stress of 0.30 MPa, the periodicity of the distortion τ, is a nearly constant value of 0.01 for these compositions. For critical blend compositions between $w = 0.60$ and 0.50, distortion is no longer present. For $w = 0.60$, a sudden drop in τ to 0.005 occurs. We must stress that this critical composition neatly coincides with that of the suspected phase inversion observed in dynamic experiments. Moreover, the vanishing of distortions is abrupt for a given shear stress, as can be seen in the extrudates presented in Fig. 7. It is clear that the addition of EVAc to mPE changes the rheological properties of mPE to such an extent that the extrusion properties are also modified. The super-slow relaxation processes observed in

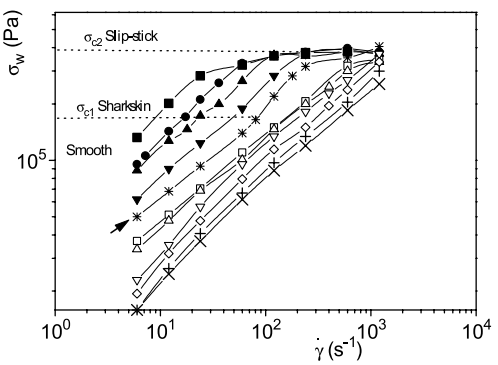

Fig. 6. Uncorrected flow curves of shear stress versus shear rate at 160 °C for the EVAc/MPE1 blends and pure materials studied (×) EVAc, (+) mPE010, (◇) mPE020, (▽) mPE030, (△) mPE040, (□) mPE050, (*) mPE060, (▼) mPE070, (▲) mPE080, (●) mPE090, (■) mPE1.

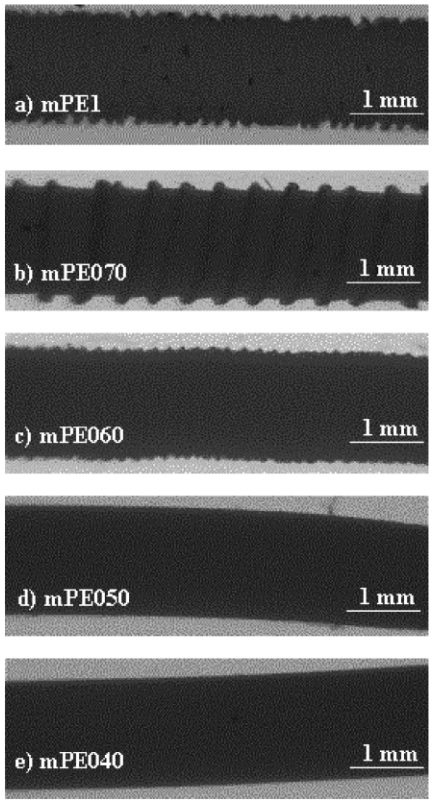

Fig. 7. Micrographs of extrudates of mPE1 and blends taken at $T = 160$ °C and $\sigma = 0.31-0.33$ MPa before the slip-stick transition (a) mPE1, (b) mPE070, (c) mPE060, (d) mPE050, (e) mPE040.

the dynamic experiments, indicate characteristic scale motion, which is significantly greater than the distance between entanglements (the interphase), associated to the deformation mechanism of the droplets. However, this factor alone is insufficient to account for the dramatic effect on extrudate appearance, thus the distortion mechanism does not disappear at high mPE contents, for which the relaxation mechanism is also observed. Distortion is only eliminated at the stage when phase inversion is suspected, that is, when EVAc becomes the system matrix. As we have pointed out in the preceding section, the EVAc is in fact no susceptible to undergo the distortion mechanism due to: (a) its higher characteristic relaxation time, (b) its higher melt strength or (c) its lower entanglement density.

4. Conclusions

The basic physical features regulating capillary flow phenomena in polyethylenes obtained by metallocene catalysts systems were explored. Our findings indicate the common behaviour of all the mPE samples analysed: the clear appearance of distortion regimes when certain critical values of shear stress are reached. Blending with ethylene/vinyl acetate copolymers gives rise to smooth extrusion for a characteristic blend composition. In this context, blends containing higher EVA levels can be suitably

extruded free of any distortion. This ideal blend composition shows good correlation with that expected for phase inversion in the system studied, i.e. when the EVAc becomes the matrix in the blend. This finding is also consistent with the IMI and the extensional deformation models. The former considers critical stress as the value for a coil-stretch transition of the layer formed by interfacial chains located at the exit of the die, and correlates the appearance of distortions with molecular dynamics. Thus, distortion only occurs if the characteristic relaxation times for the entanglement–disentanglement process are of the order of the inverse of the shear rate window involved in the extrusion experiments, as in the case of linear mPEs of moderate polydispersity index. Being branched, and in contrast to the mPEs, the EVA copolymer is characterised by long relaxation times, and does not, therefore, develop distortions during extrusion. The extensional deformation model considers a critical value for the product of the extensional strain rate and the total strain at the exit-die region. It is obvious that when the material is characterised by a high melt strength (as occurs with long chain branched polymers) this critical product increases, and distortions may not occur. It would be also of interest to consider the possibility of a lower entanglement density in EVAc as the cause of the elimination of the distortions.

It follows that at and beyond the phase inversion concentration, flow is dominated by the long branched EVA copolymer, so the characteristic sharkskin phenomenon of the extrudate no longer occurs, whichever the distortion mechanism.

Acknowledgements

Thanks are due to the CICYT (Grant MAT2002-01242) for supporting this investigation. The authors also acknowledge Repsol-YPF (Spain) for their permission to publish these data.

References

[1] Kim YS, Chung CI, Lai SY, Hyun KS. ANTEC'95 1995, 1122.
[2] Kim YS, Chung CI, Lai SY, Hyun KS. J Appl Polym Sci 1996;59:125.
[3] Kim YS, Chung CI, Lai SY, Hyun KS. Korean J Chem Engng 1996; 13:294.
[4] Vega JF, Fernández M, Santamaría A, Muñoz-Escalona A, Lafuente P. Macromol Chem Phys. 1999;200:2257.
[5] Tapadia PS, Joshi YM, Lele AK, Maselkar RA. Macromolecules 2000;33:250.
[6] Pérez-González J, de Vargas L, Pavlínek V, Hausnerová B, Sáha P. J Rheol 2000;44:441.
[7] Ghanta VG, Riise BL, Morton MM. J Rheol 1999;43:435.
[8] Moynihan RH, Baird DG, Ramanathan R. J Non-Newt Fluid Mech 1990;36:255.
[9] Piau JM, Nigen S, El Kissi N. J Non-Newt Fluid Mech 2000;91:37.
[10] Hong Y, Cooper-White J, Mackay ME. J Rheol 1999;43:781.
[11] La Mantia FP, Geraci G, Vince M, Pedretti U, Roggero A, Minkova LI, Magagnini PL. J Appl Polym Sci 1995;58:911.
[12] Kolnaar JWH, Keller A. J Non-Newt Fluid Mech 1997;69:71.
[13] Aguilar M, Vega JF, Muñoz-Escalona A, Martínez-Salazar J. J Mater Sci 2002;37:3415.
[14] Kazatchov I, Yip F, Hatzikiriakos SG. Rheol Acta 2000;39:583.
[15] Cogswell FN, Barone JR, Plucktaveesak N, Wang SQ. J Rheol 1999; 43:245.
[16] Howells ER, Benbow JJ. Trans J Plast Int 1962;30:240.
[17] Bartos O, Holomek J. Polym Engng Sci 1971;11:324.
[18] Cogswell FN. J Non-Newt Fluid Mech 1977;2:37.
[19] El Kissi N, Piau JM, Toussaint F. J Non-Newt Fluid Mech 1997;68: 271.
[20] Rutgers R, Mackley M. J Rheol 2000;44:1319.
[21] Kalika DS, Denn MM. J Rheol 1987;31:815.
[22] Hatzikiriakos SG, Dealy JM. J Rheol 1992;36:703.
[23] Black WB, Graham MD. Phys Rev Lett 1996;77:956.
[24] Hill DA. J Rheol 1998;42:581.
[25] Brochard F, de Gennes PG. Langmuir 1992;8:3033.
[26] Wang SQ, Drda PA. J Rheol 1996;40:875.
[27] Wang SQ, Drda PA. Macromol Chem Phys 1997;198:673.
[28] Migler KB, Son Y, Qiao F, Flynn K. J Rheol 2002;46:383.
[29] Peón J, Vega JF, Martínez-Salazar J. Submitted for publication, 2002.
[30] Peón J, Vega JF, Aroca M, Martínez-Salazar J. Polymer 2001;42: 8093.
[31] Aguilar M, Vega JF, Sanz E, Martínez-Salazar J. Polymer 2001;42: 9713.
[32] Lacroix C, Grmela M, Carreau PJ. J Rheol 1998;42:41.
[33] Cox WP, Merz EH. J Polym Sci 1958;28:619.
[34] Milner ST. J Rheol 1996;40:303.
[35] Utracki LA, Schlund B. Polym Engng Sci 1987;27:1512.
[36] Steinman S, Gronski W, Friedrich C. Rheol Acta 2002;41:77.
[37] Utracki LA. J Rheol 1991;35:1615.
[38] Krieger IM, Dougherty TJ. Trans Soc Rheol 1959;3:137.
[39] Fernández M, Vega JF, Santamaría A, Muñoz-Escalona A, Lafuente P. Macromol Rapid Commun 2000;21:973.
[40] Deeprasertkul C, Rosenblatt C, Wang SQ. Macromol Chem Phys 1998;199:2113.
[41] Yang X, Ishida H, Wang SQ. J Rheol 1998;42:63.
[42] de Gennes PG. Scaling concept in polymer physics. Ithaca, NY: Cornell University Press; 1979.
[43] Hatzikiriakos SG. Polym Engng Sci 2000;40:2279.
[44] Wood-Addams P, Dealy JM. Macromolecules 2000;33:7481.
[45] Tapadia S, Joshi YM, Lele AK, Mashelkar RA. Macromolecules 2000;33:250.
[46] Yamaguchi M, Miyata H, Tan V, Gogos CG. Polymer 2002;43:5249.
[47] El Kissi N, Piau JM, Toussaint F. J Non-Newt Fluid Mech 1997;68: 271.